Effect of Humidity on Reverse Breakdown in 3D Silicon Sensors for Particle Tracking

Haley McDuff

Department of Physics and Astronomy, University of New Mexico, Albuquerque, NM 87131, USA

April 25, 2014

Abstract

An important parameter in characterizing and operating a 3D sensor is its breakdown voltage. In this study we examine the effects of ambient humidity on 3D sensor breakdown. Leakage currents and breakdown voltages are measured as a function of humidity for constant temperature over a range of relative humidities and bias voltages. These effects are studied for unirradiated and irradiated samples exposed to fluences relevant to the environment of the High Luminosity Large Hadron Collider. The proton beam at LANSCE, Los Alamos National Laboratory, was used to irradiate certain samples with 800 MeV protons up to 1×10^{16}p/cm^2.

Contents

Chapter 1

Silicon Particle Sensors

1.1 Silicon as a Semiconductor

A semiconductor is a material with conductivity between that of an insulator and a conductor. Most semiconductors are single crystals with each atom forming covalent bonds by sharing all of its valence electrons with neighboring atoms. One semiconductor often used in particle sensors is silicon [1], which has four valence electrons. The electrons in the atoms have a large number of energy states which they can inhabit. The various energy states are very closely spaced, forming virtually continuous energy bands which may be separated by energy gaps. There is a gap between the valence band and the next higher-energy band, which is known as the conduction band. The electrical behavior of a material depends on its band-gap structure. The structures of a semiconductor, insulator and conductor are shown in Figure 1.1.

A semiconductor has a gap between the valence band and the conduction band that is greater than that of a conductor, but smaller than that of an insulator. At low temperatures, the valence electrons in the semiconductor will occupy the lower energy states, filling up the valence band and allowing the material to act as an insulator. At higher temperatures electrons are excited into the conduction band where they are free to flow, allowing the material to act as a conductor. In silicon, the bandgap between the valence and conduction bands is 1.12 electron volts; i.e. an electron in

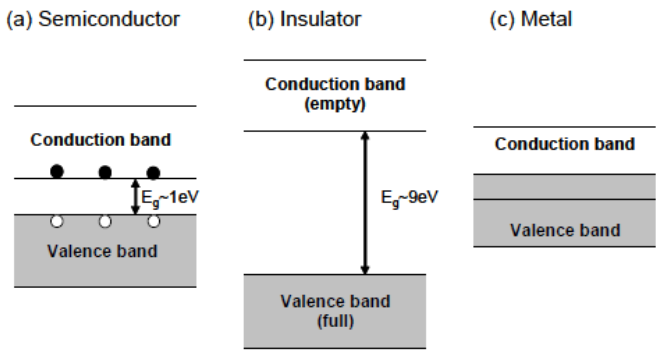

Figure 1.1: Band structures of a (a) semiconductor, (b) insulator, (c) conductor.

the valence band of an atom in a silicon crystal lattice must receive 1.12 eV of energy in order to be excited into the conduction band. Insulators have a similar band structure but with a wider bandgap, so more energy is needed to excite the electrons into the conduction band. Conductors have essentially no bandgap between the valence and conduction bands allowing charges to move freely, even at low temperatures.

1.2 Silicon p-n Junction

Silicon particle sensors typically include at least one p-n junction [2]. Silicon can be doped by replacing a desired concentration of silicon atoms within the silicon crystal lattice with atoms of other elements. N-type silicon has been doped with atoms with five valence electrons (such as phosphorous), four of which form covalent bonds with the surrounding silicon atoms while the fifth electron remains loosely bound and can easily be excited into the conduction band. In fact, nearly all of these loosely bound electrons inhabit the conduction band at room temperature. P-type silicon is doped with atoms that only have three valence electrons and the ability to hold a fourth, such as boron. This leaves free positive space charges, or holes, when the doping atoms form covalent bonds with the surrounding lattice of silicon atoms.

A p-n junction is formed by doping an n-type region and a p-type region next to each other in a silicon substrate. The free electrons from the n-type then diffuse toward the holes within the

p-type silicon, and the free holes from the p-type migrate toward the n-type silicon until a steady state is attained, as shown in Figure 1.2. As both positive and negative charges diffuse across the boundary, they begin to induce a net electric field, called a built-in field, which causes a drift current of free charges that opposes the initial direction of diffusion. When the built in field lies antiparallel to the initial electric field caused by the polarity of the n-type and p-type materials, the charges stop drifting and the steady state is formed. This leads to a space of effectively intrinsic silicon between the n-type and p-type silicon. This space contains no free charges and is known as a depleted region.

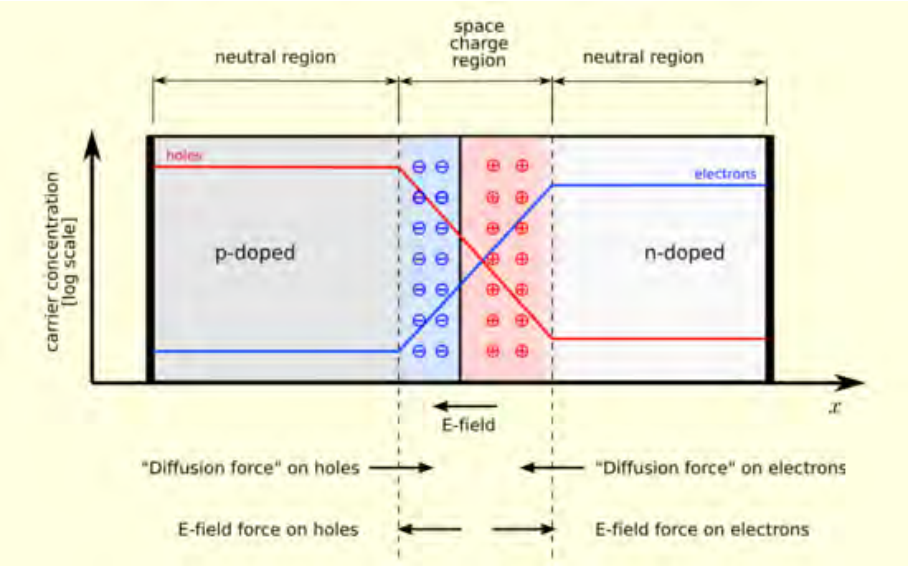

Figure 1.2: When no external bias voltage is applied, the electric field induced by the charges that have diffused across the p-n junction counteracts the initial electric field caused by the polarity of the n-type and p-type materials, the charges stop drifting and the steady state is formed.

The width of the depletion region can be controlled by applying a voltage across the p-n junction as seen in Figure 1.3. A forward bias (lower electric potential is applied to the n-type silicon) causes the width of the depletion region to decrease. A reverse bias (lower electric potential applied to the p-type silicon) causes the width of the depletion region to increase. By reverse biasing the p-n junction, the increased depletion region restricts the amount of current through the junction and provides a nearly uniform electric field throughout the entire sensor, which is a key component for

use in particle sensors.

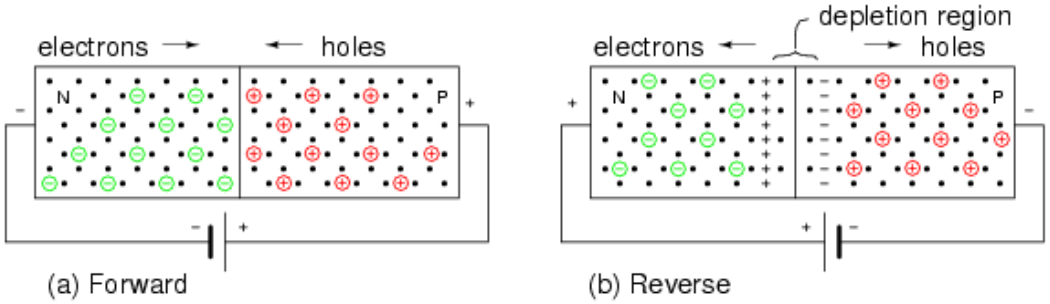

Figure 1.3: Forward and reverse biasing effects on the p-n junction.

1.3 Application to Particle Sensors

Particle sensors that utilize p-n junctions in high energy physics are typically operated with a reverse bias as this reduces the amount of noise from dark current and creates a large volume devoid of free charge carriers. The high electric field allows for quick signal collection. Some applications require fast charge collection, such as particle tracking in experiments at the LHC where particle collisions occur every 25 ns. When the reverse bias is applied, it creates an electric field through the body of the sensor between the electrodes (electrified p^+ and n^+ regions). When an energetic particle travels through the silicon, it liberates a trail of electron-hole pairs along its path by exciting electrons in the silicon atoms into the conduction band. The free electrons and holes then drift toward the electrodes which have the bias voltage applied. When the drifting charges reach the electrodes, they induce a current pulse which can then be measured.

1.4 3D Geometry

Traditional silicon particle sensors consist of a slab of lightly doped silicon with a usually asymmetrical orientation of more highly doped p-type (p^+) and n-type (n^+) material acting as electrodes on either surface of the silicon body of the sensor. The 3D geometry was proposed in 1997 [3]

specifically to perform within the extreme radiation environment of contemporary hadron colliders. Unlike planar sensors which utilize strips or planes of n^+ and p^+ silicon on the surface of the silicon bulk of the sensor, 3D sensor p^+ and n^+ electrodes are etched into the body of the sensor and filled with the dopant material. Depending on the design, the n-type and p-type electrodes may extend partway through the bulk of the sensor or penetrate all the way through the substrate. A comparison of planar and 3D geometries is shown in Figure 1.4.

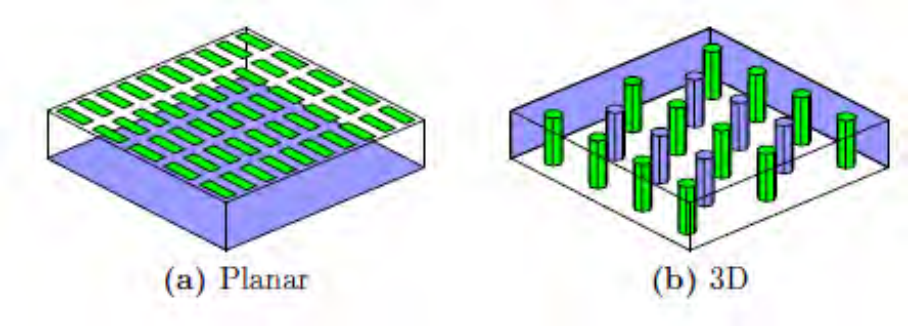

Figure 1.4: Planar sensors place electrodes on either surface of the body of the sensor. In the 3D geometry, electrodes are inserted into the body of the sensor.

An active edge 3D sensor utilizes trenches in the silicon bulk that trace the perimeter of the sensor refCinzia. These trenches are filled with active material (n-type or p-type Si). The trenches are biased along with the electrodes, creating an electric field parallel to the sensor's surface and depleting any areas within the body of the sensor that would otherwise be dead space. This allows sensors to be tiled side-by-side with minimal loss of active regions within the sensors, rather than having to be overlapped to compensate for the perimeter of inactive bulk in sensors without an active edge.

The primary benefit of the 3D geometry is that, for the same number of liberated electron-hole pairs, there is less distance between the p^+ and n^+ electrodes, on the order of 10^1 μm as opposed to 10^2 μm for planar sensors (see Figure 1.5). The reduced electrode spacing of the 3D sensors requires less voltage to deplete the body of the sensor, allows free charges to be collected faster, and reduces the probability of charges getting trapped by defects in the silicon crystal. Charge trapping by irregularities in the silicon becomes more significant as the sensor is exposed to radiation at, for

example, the LHC. Exposure to radiation physically damages the silicon crystal which inhibits the smooth flow of charges to the electrodes thereby increasing the data collection time.

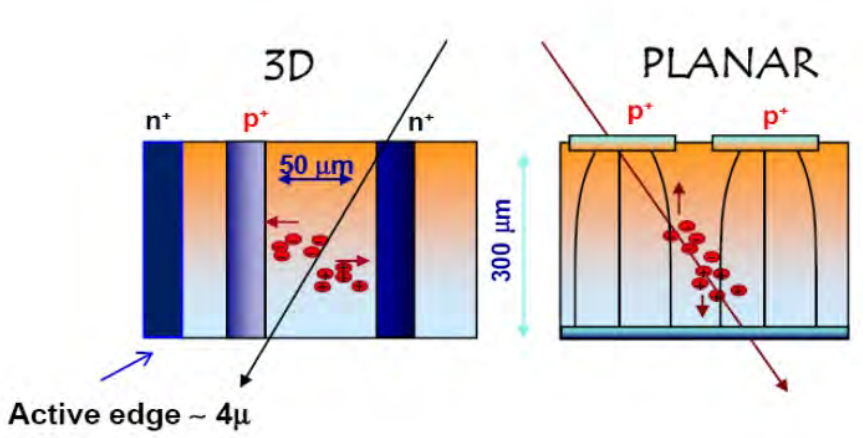

Figure 1.5: Energetic particles generates a trail of free electron-hole pairs that drift toward the electrodes.

Any surface of silicon that comes on contact with oxygen will oxidizes to form a layer of silicon dioxide (SiO_2) over the exposed surface of the sensor. There is a presence of positive oxide charges in the SiO_2 layer which may be due to holes trapped in defects within the oxide [4]. These positive charges induce a layer of negative charges within the bulk of the sensor at the Si-SIO_2 interface.

1.5 Sensor Measurements

The primary measurement used in the characterization of 3D sensors is leakage current versus bias voltage (IV). To perform an IV measurement, the leakage current through the sensor is measured as the reverse bias voltage across the p^+ and n^+ electrodes is incremented from 0 V until breakdown occurs. Breakdown is characterized by the rapid increase of leakage current (primarily due to carriers being excited through the bandgap) while the sensor is under reverse bias. The bias voltage that corresponds to this effect is the breakdown voltage. Breakdown does not actually damage the sensors as long as current levels are limited such that the silicon is not allowed overheat. As the sensor begins to break down with increasing reverse bias voltage, the magnitude of the leakage

current begins to increase rapidly, see Figure 1.6.

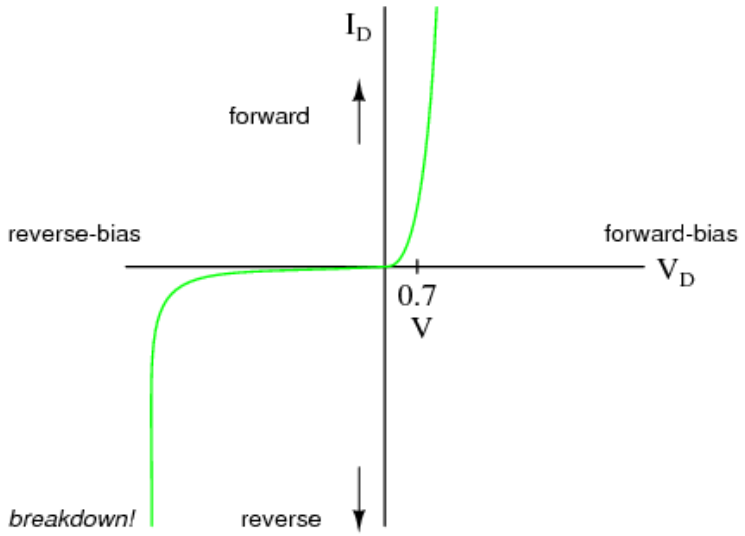

Figure 1.6: Bias voltage versus leakage current. As the sensor begins to breakdown with increasing bias voltage, the magnitude of the leakage current begins to increase exponentially .

A high breakdown voltage is desirable because it allows for a large range of operation voltages while the leakage current remains approximately constant over a greater range of bias voltages. To determine the quality of performance of the 3D sensors, IV measurements are taken before and after the sensors are irradiated with fluences relevant to their operational environment. Radiation damages the crystal lattice of the silicon within the sensor which allows more current to flow through the bulk of the sensor, even when fully depleted.

1.6 Motivation for the Study

Results from a recent study [5] showed evidence of a humidity dependence on the breakdown voltage of 3D sensors and provided a possible explanation. However, because the humidity effects were not the focus of the study, it lacked enough data to support the conclusion. In order to explore the humidity phenomena, IV measurements were taken on FBK-style 3D sensors [6] provided by collaborators at the University of Trento, Italy. The results are shown in Figure 1.7. The sensors

named FEI-1RMC-2 in Figure 1.7(a) and FEI-1R2C-1 in Figure 1.7(b) are non-irradiated and FEI4-#3 in Figure 1.7(c) has been irradiated with 800 MeV protons to 5×10^{15} 1-MeV-neutron-equivalent (neq). The sensors were held at a constant temperature and the relative humidity (RH) of the environment around the sensor was incremented in steps of approximately 10% from 0.1% RH (with dry nitrogen blowing over the sensor) to 80% RH.

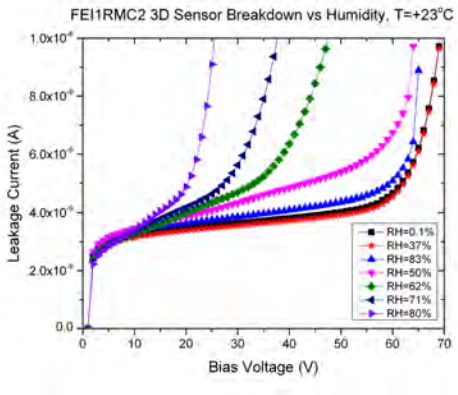

(a) Sensor FEI-1RMC-2, un-irradiated.

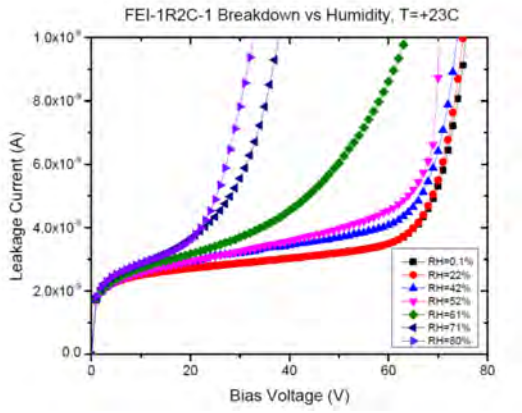

(b) Sensor FEI-1R2C-1, un-irradiated.

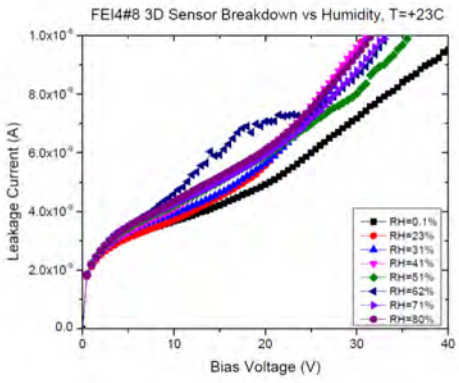

(c) Sensor FEI4-#3, irradiated, 5×10^{15} neq.

Figure 1.7: As humidity is increases from 0.1% to 80%, the leakage current increases and the breakdown voltage seems to decrease.

There is a clear humidity dependence on the apparent breakdown of the sensors, but this brief study did not provide enough information about the increased level of leakage current with increased humidity. It could not be made clear whether or not the hypothesized increased surface currents

lead to the breakdown of the sensor or if breakdown remained a characteristic of the bulk of the sensor. The need for more specific data prompted the study discussed in the following chapter.

Chapter 2

Study: Humidity Dependence of IV Measurements in 3D Silicon Sensors

3D silicon sensors [3, 5] have potential applications in a wide range of fields, but most notably they are planned or under consideration for use in several experiments at the Large Hadron Collider (LHC) and High Luminosity LHC (HL-LHC) because of their radiation hardness. The environment in which 3D sensors will be used in ATLAS is well-controlled below 0°C with relative humidity effectively zero in a dry N_2 environment [7]. Outside the controlled environment of the experiments, in beam tests and during planned and unplanned warm-ups, the effects of humidity upon the performance of the sensors must be anticipated. Additionally the humidity response of the sensors must be considered when developing plans for future cooling methods.

It is known that surface charges can affect the behavior of silicon sensors. Charges from the external sensor environment, including negative charges associated with humid air, travel along electric field lines that loop outside the sensor between the n and p electrodes to the SiO_2 layer, until groups of charges aggregate around electrodes of opposite sign [5]. This can increase the

magnitude of the electric field around the electrodes and potentially cause localized breakdown to occur [8]. Such electron drift has been shown in simulations [3]. The silicon oxide layer on the sensor can also induce a thin accumulation layer of negative charges from the environment which compensates for some of the positive charges within the SiO_2. Continuing to increase negative charges along the oxide surface can cause instabilities in the leakage current and eventually lead to surface depletion, thereby increasing the total leakage current of the sensor [9].

Studies have been made of the effect of humidity on capacitance [8, 10] and leakage current and breakdown [9, 11] in planar strip sensors. Data on humidity effects on 3D geometries is not readily available in the literature. In this study, 3D sensor breakdown and leakage current (I_L) are examined as a function of humidity for constant temperature.

2.1 Devices

The devices [12], manufactured at SLAC, are 3D sensors in n-type bulk with active edges [13]. Figure 2.1 shows their layout. Three signal electrodes are in each 50 μm x 400 μm pixel [5]. The edge region is made with a perimeter trench filled with n^+ silicon, making the sensor efficient to within a few microns of the physical edge [12]. The sensors are arranged with separate edge-biasing pads and electrode readout pads which allow simultaneous readout of two leakage currents. The edge-biasing pads provide the total leakage current, which includes contributions from the electrodes, surface, and active edges of the sensor. The electrode readout pads are insulated from any active-edge or surface currents which allows them to read out the electrode leakage current only. Three unirradiated sensors are measured (Sensor1, Sensor2, and Sensor3) as well as two sensors irradiated at the LANSCE facility, Los Alamos National Laboratory, with 800 MeV protons to fluences 2×10^{15} (Sensor4) and $1 \times 10^{16} p/cm^2$ (Sensor5). As the hardness factor of these protons is 0.71, these fluences are equivalent to 1.4 and 7×10^{15} 1 MeV neutron equivalent (neq) respectively. These fluences are relevant for the ATLAS Insertable B-Layer (IBL) and other future LHC tracking upgrades.

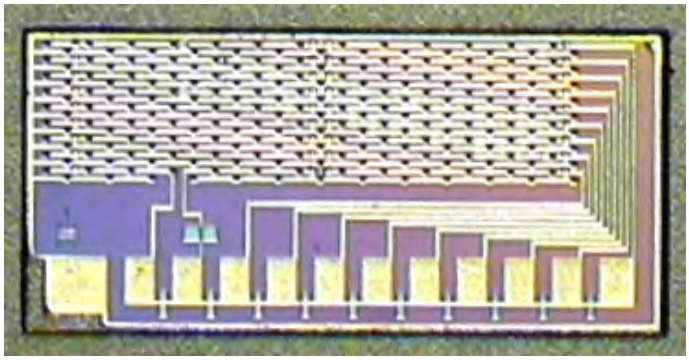

Figure 2.1: A photograph of one of the sensors. The readout pads are all joined together. A negative bias voltage is applied to the bias pad, visible on the righthand side below the readout pads row, to deplete the device.

2.2 Setup

The setup for measuring leakage currents and sensor breakdown as a function of humidity is shown in Figure 2.2. Reverse bias voltage (V_{bias}) is applied to the sensor's edge pad with the Keithley 237 Source Measure unit, which also provides the measurement of the total (electrode, surface, and edge) current. The electrode leakage current is measured separately with the Keithley 617 Electrometer. The thermal chuck on which the sensor rests maintains a constant temperature (20°C or 24°C for unirradiated sensors, 10°C for irradiated sensors,) to within ±1.3%. The humidity generator saturates the environment around the sample with water vapor by passing dry air - of approximately 10% (RH) - over water within an enclosed reservoir, then flowing the air over the sensor. Relative humidities less than 10% RH are produced by flushing the sensor environment with a controlled flow of N_2. Relative humidity is monitored with a Sensirion Model SHT71 humidity detector within the sensor environment.

2.3 Procedure

To study their operational stability over time, the sensors are held for 7-8 hours at 40% RH with measurements of leakage current versus bias voltage (IV) taken approximately once per hour. Both leakage currents (total and electrode) are measured while the sensors are reverse biased, with

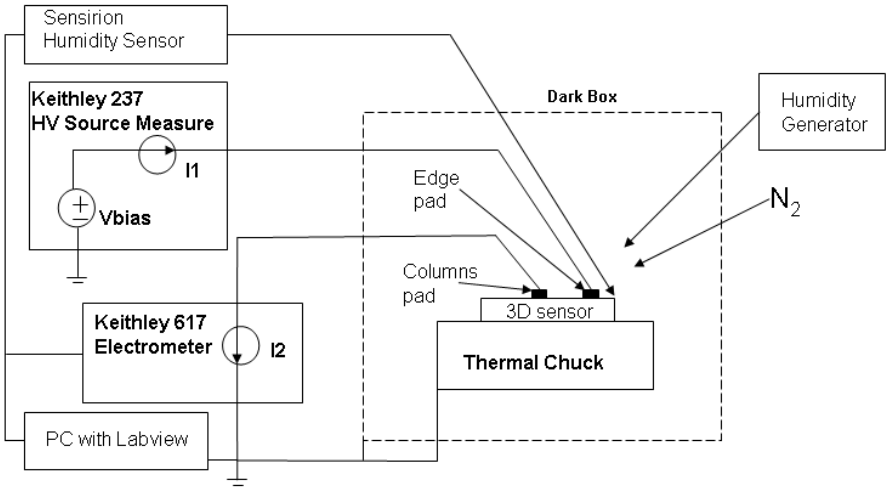

Figure 2.2: The experimental setup for measuring leakage current as a function of bias voltage for controlled humidity variations.

V_{bias} ramped up in 1 volt increments from 0 V until breakdown occurs. For the purposes of this study, breakdown voltage is determined as the V_{bias} step after the leakage current reaches three times the value of the current at the midpoint of the stable current region. To measure current and breakdown voltage versus relative humidity, two IV's are measured simultaneously. The measurements are repeated as the relative humidity of the sensor environment is varied from 0.1% to 80% in approximately 5% increments.

2.4 Experimental Results

2.4.1 Stability

As is shown in Figure 2.3, Sensor1 maintains a breakdown voltage of 80V±2V at RH=40% and 100V±2V at RH=0.1%, and Sensor2 maintains a breakdown voltage of 49V±1.5V at RH= 40%. No significant breakdown voltage instability with time is observed for up to 7 hours.

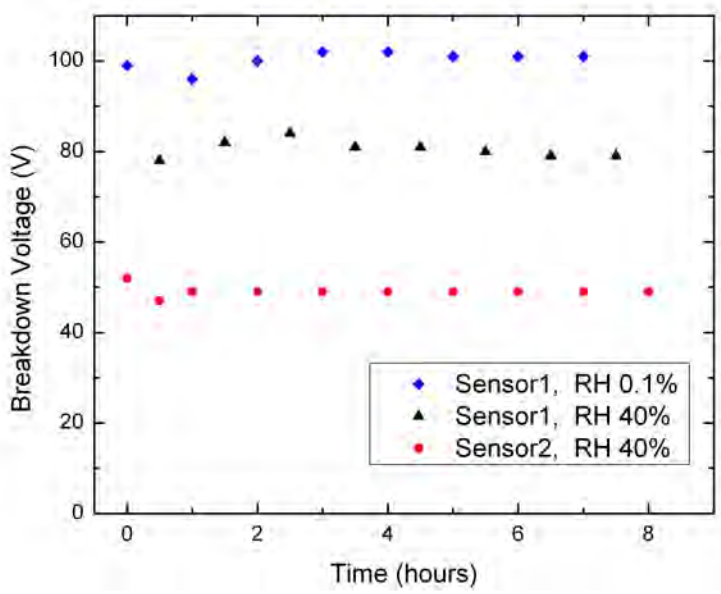

Figure 2.3: Breakdown voltage as a function of time for two humidity conditions. The size of the symbols covers the uncertainty in the measurement.

2.4.2 Leakage Current

Two sets of IV curves are measured for (unirradiated) Sensor1. Figure 2.4 (a) shows the *electrode* leakage current at 24°C as a function of bias voltage for eleven levels of relative humidity. Below breakdown, the current is independent of humidity. Figure 2.4 (b) shows the *total* leakage current for the same conditions. As relative humidity varies from 13% to 65%, the total leakage current increases by more than an order of magnitude. The total leakage current from Sensor2 triples as the humidity increases from 0.1% to 65%, and the total current from Sensor3 doubles as the humidity changes from 0.1% to 80%.

The same features are seen in Figure 2.5 for (irradiated) Sensor5 with leakage current up to nearly five times higher at 50% RH than at 0.1% RH. The leakage current of Sensor4 increases by a factor of 1.5 as humidity increases from 0.1% RH to 70% RH. These results are summarized in Table 2.1.

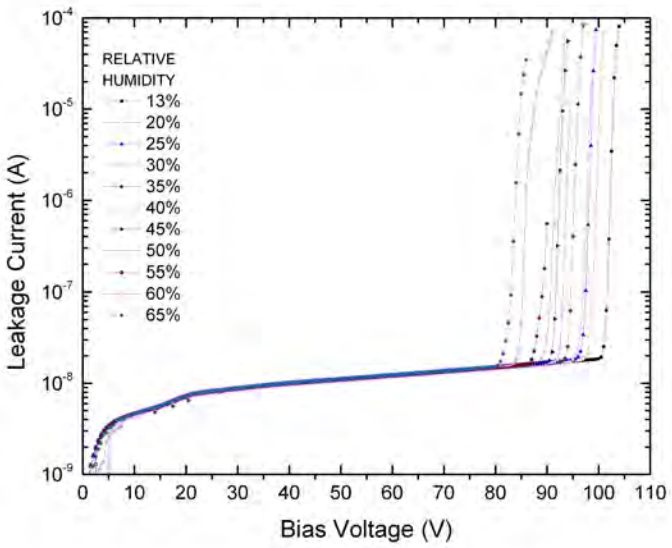

(a)

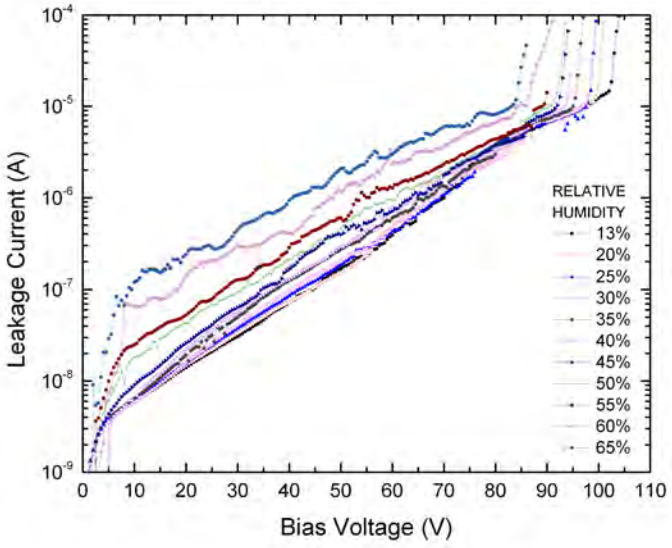

(b)

Figure 2.4: Sensor1 electrode (a) and total (b) leakage current as a function of bias voltage, at constant temperature of 24°C, for eleven levels of relative humidity from 13% to 65%.

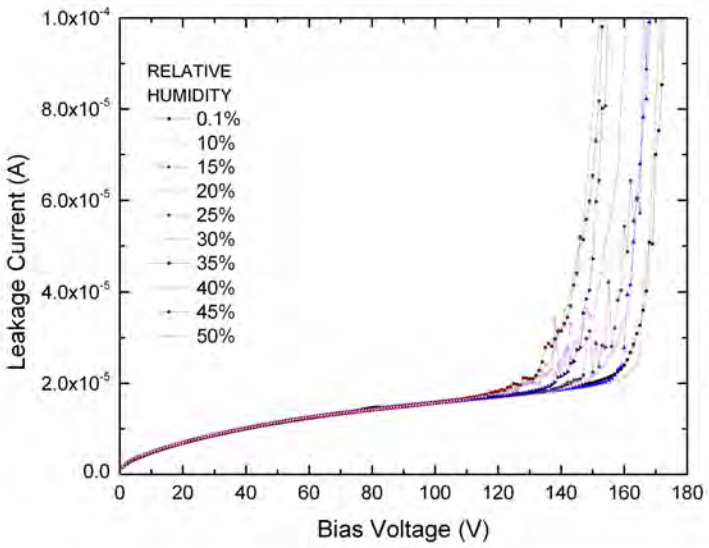

(a)

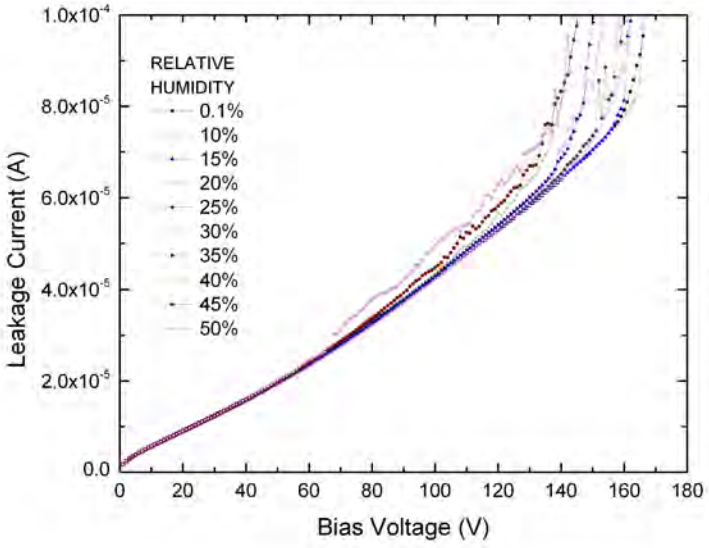

(b)

Figure 2.5: Sensor5 electrode (a) and total (b) leakage current as a function of bias voltage, at constant temperature of 10°C, for ten levels of relative humidity from 0.1% to 50%.

	Current Increase Factor (I_+)	ΔV_{BD} (V)	Humidity Range (RH)
Sensor1	10	18	13%-65%
Sensor2	3	26	0.1%-65%
Sensor3	2	31	0.1%-80%
*Sensor4	1.5	54	0.1%-70%
*Sensor5	5	25	0.1%-50%

Table 2.1: As the relative humidity increases from minimum to maximum values for each sensor's respective humidity range, the total leakage current increases by a factor of I_+, and the electrode breakdown voltage decreases by ΔV_{BD}. Irradiated sensors are indicated by *.

2.4.3 Electrode Breakdown Voltage

Figure 2.4(a) also shows a sharp "knee" in the region of the bias breakdown voltage. As the relative humidity increases, the knee moves to the left; i.e, the electrode breakdown voltage decreases. The breakdown voltage for Sensor1 decreases from 101 V at 13% RH to 83 V at 65% RH. The breakdown voltage of Sensor2 decreases from 86 V to 60 V as humidity increases from 0.1% to 65% RH, and the breakdown voltage of Sensor3 decreases from 108 V to 77 V as humidity increases from 0.1% to 80% RH. The same effect is seen in the irradiated sensors. Figure 2.5(a) shows the electrode breakdown of Sensor5 decreasing from 168 V to 143 V as humidity increases from 0.1% to 50% RH. The breakdown voltage of Sensor4 decreases from 178 V to 124 V for humidity increasing from 0.1% to 70% RH. (Note that proton irradiation increases the breakdown voltage of this sensor geometry by approximately 60 V regardless of humidity). These results are also summarized in Table 2.1.

2.4.4 Systematic Uncertainties

Errors intrinsic to the setup configuration include uncertainties produces by probe placement and data being taking at 1 volt increments. Probe placement error was calculated by systematically measuring the IV of a sensor under the same conditions ten times, re-placing the measurement probes each time. The fluences are known to precision 10-15%.

Uncertainties	Leakage Current	Breakdown Voltage
Keithley 237	$\pm(0.035\% + 60\text{nA})$	$\pm(0.033\% + 24\text{mV})$
Keithley 617	$\pm(0.25\% + 10\text{pA})$	-
Temperature $\pm 0.3^{\circ}$C	0.5%	± 0.2 V
Setup Configuration	1.89%	± 1 V
Total	1.97%	$< 3\%$

Table 2.2: Source and values of errors on leakage current and breakdown voltage.

Leakage Current Error

The systematic uncertainties on leakage current from the manufacturer's accuracy specifications are $\pm(0.035\% + 60\text{nA})$ for the Keithley 237 and $\pm(0.25\% + 10\text{pA})$ for the Keithley 617. Temperature variations of $\pm 0.3^{\circ}$C produce an error in leakage current of 0.003%. The leakage current error from the setup configuration was calculated at 60 V and is 1.89%. The total systematic uncertainty on the leakage current is 1.95%

Breakdown Voltage Error

The systematic uncertainty on the bias voltage from the manufacturer's accuracy specifications is $\pm(0.033\% + 24\text{mV})$ for the Keithley 237. Variation in temperature produces an uncertainty in breakdown voltage of ± 0.2 V. Error on the breakdown voltage due to the bias voltage step size ± 1 V. The total uncertainty on the breakdown voltage is less than 5%. A summary of sources of errors and error values is shown in Table 2.2.

2.5 Conclusions

Reverse breakdown in 3D silicon sensors has been examined over a range of relative humidity from 0.1% to 80% for both irradiated and unirradiated samples. The point of breakdown is shown to be stable, regardless of relative humidity, over a period of up to 8 hours. Total leakage current increases by a factor of 2 to 10 as relative humidity is raised from a few percent to 50% or higher, independent of fluence received. The substantial increase in total current manifests in the edge and

surface currents and produces no observed early breakdown phenomena on the electrode current. The electrode leakage current remains unaffected by changes in relative humidity, but the electrode breakdown voltage decreases by approximately 20-30% as relative humidity is raised from a few percent to 50% or higher.

2.6 Acknowledgements

A special thank you to Martin Hoeferkamp and Rui Wang for their vital contributions to this study, and to Dr. Sally Seidel for her mentorship and providing me with this research opportunity. I would also like to thank Sherwood Parker and Chris Kenney for providing the 3D sensors. This work was supported by the U.S. Department of Energy and the National Science Foundation.

Bibliography

[1] S. M. Sze, Physics of Semiconductor Devices, John Wiley & Sons, 1981.

[2] Ben G. Streetman Solid State Electronic Devices, Prentice Hall, 1990.

[3] S.I. Parker, C.J. Kenney, J. Segal, Nucl. Instr. and Meth. A 395 (1997) 328-343.

[4] Gerhard Lutz Semiconductor Radiation Detectors, Springer-Verlag, 1999.

[5] Sherwood Parker, et al., Nucl. Instr. and Meth. A 685 (2012) 98-103.

[6] Cian-Franco Dalla Betta, et al., IEEE, 2013. Proceedings of: NSS-MIC 2013, Seoul, Corea del Sud, 27 ottobre - 2 novembre 2013

[7] R. Hawkings, Humidity Control in the ATLAS ID, talk given at JCOV meeting, CERN, 18 March 2004.

[8] A. Longoni, M. Sampietro, L. Struder, Nucl. Instr. and Meth. A 288 (1990) 35-43.

[9] M. Laakso, P. Singh, P.F. Shepard, Nucl. Instr. and Meth. A 327 (1993) 517-522.

[10] A. Chilingarov, D. Campbell, G. Hughes, Nucl. Instr. and Meth. A 560 (2006) 118-121.

[11] F. G. Hartjes, Nucl. Instr. and Meth. A 552 (2005) 168-175.

[12] Cinzia DaVia, Mario Deile, et al., IEEE Transactions on Nuclear Science 56 (2009) 505.

[13] C. J. Kenney, et al., Nucl. Instr. and Meth. A 565 (2006) 272-277.